BANDELET-BASED ANISOTROPIC DIFFUSION

Aldo Maalouf, Philippe Carré, Bertrand Augereau, Christine Fernandez-Maloigne

University of Poitiers
Signal-Image-Communication Laboratory
SP2MI-2 Bd Marie et Pierre Curie, PO Box 30179
86962 Futuroscope Chasseneuil, France
{maalouf, carre, augereau, fernandez}@sic.sp2mi.univ-poitiers.fr

ABSTRACT

Visual tasks often require a hierarchical representation of images in scales ranging from coarse to fine. A variety of linear and nonlinear smoothing techniques, such as Gaussian smoothing, anisotropic diffusion, regularization, wavelet thresholding etc... have been proposed. In this work, we propose a geometrical multiscale anisotropic diffusion based on the geometrical flow for denoising multivalued images. The geometrical flow is determined by the Bandelet transform of the image being processed. Consequently, the image is segmented into a quadtree where each square regroups pixels sharing the same geometrical flow direction. The motivation of this work is to introduce a new multiscale multistructure bandelet-based diffusion tensor to adjust the anisotropic diffusion toward the direction of the optimal geometrical flow. Therefore, multiple dyadic squares in the quadtree have multiple structure tensors. Hence, a more accurate geometrically driven noise suppression is obtained where the homogeneity of different image regions is well maintained.

Index Terms— Bandelet, wavelet, anisotropic diffusion, filtering, color images

1. INTRODUCTION

An observed digital image can contain random noise η superimposed on the pixel intensity by the following formula:

$$I_{noisy} = I_{true} + \eta \tag{1}$$

We would like to recover the true image I_{true} from its noisy observation I_{noisy}. Noise is recognized as rapidly oscillating signals and can, therefore, be removed by the process of low-pass filtering at the expense of some details such as edges. Wavelet-based methods, statistical methods, and diffusion filters have successfully been used to remove noise from digital images. In applications, a number of authors stick to the original Perona-Malik's anisotropic diffusion scheme [1], but numerous derived, similar and/or improved, algorithmic approaches have appeared in the meantime. Novel application areas for anisotropic diffusion have emerged which prove the power of these filters for both 2D and 3D data filtering. This makes the need for amelioration of the anisotropic diffusion a challenging task.

The Bandelet transform was firstly introduced by Le Pennec and Mallat [2]. The first generation of Bandelet basis was not built directly in the discrete domain and therefore it does not provide a multiresolution representation of the geometry. Furthermore, the first generation of Bandelet showed some edge artifacts that are undesirable in an edge preserving diffusion scheme. On the other hand, the second generation of Bandelet transform, introduced by Peyre and Mallat in [3], is computed with a geometric orthogonal transform that is applied on orthogonal wavelet coefficients. Thus, each geometric direction leads to a different transform.

Taking advantage of this geometrical representation, a multispectral multistructural tensor is proposed to adjust the image gradient in the denoising process toward the geometry direction. Given that the singularity of edges is well presented in the Bandelet basis by elongated functions that are nearly parallel to these edges and that the image pixels sharing the same geometrical properties are distributed on different dyadic squares defined by the direction of the geometrical flow, an accurate edge-preserving, less blurring and homogeneity maintaining anisotropic diffusion is obtained.

The rest of the paper is organized as follows. In section 2, a review of the Bandelet transform is presented. In section 3, a description of the Perona-Malik diffusion scheme is given. In section 4, the bandelet-based anisotropic diffusion is described. Experimental results are shown in section 5 and section 6 presents some concluding remarks.

2. BANDELET TRANSFORM

We only present here a brief review of the Bandelet transform. The reader can refer to [4] for a full detailed description of the Bandelet transform.

The bandelets are defined as anisotropic wavelets that are warped along the geometric flow, which is a vector field indicating the local direction of the regularity along edges. The dictionary of bandelet frames is constructed using a dyadic square segmentation and parametrized geometric flows. The ability to exploit image geometry, makes its approximation error decay optimal asymptotically for piece-wise regular images.

For image surfaces, the geometry is not a collection of discontinuities, but rather areas of high curvature. The Bandelet transform recasts these areas of high curvature into an optimal estimation of regularity direction. Figure 1 shows an example of bandelets along the geometric flow in the direction of edges. In real applications, the geometry is estimated by searching for the regularity flow and then for a polynomial to describe that flow.

2.1. Implementation of the Bandelet Transform

The Bandelet transform is first implemented by reordering the 2D Wavelet coefficients and then performing a 1D wavelet transform. The classical tensor wavelet transform of an image I is the

This work was supported by the INTERREG III B PIMHAI project.

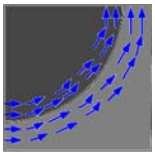

Fig. 1. An illustration of bandelets with geometric flows in the direction of the edge. The support of the wavelets is deformed along the geometric flows in order to exploit the edge regularity.

decomposition of the latter on an orthogonal basis formed by the translation and dilation of three mother wavelets $\{\psi^H, \psi^V, \psi^D\}$ for the horizontal, vertical and diagonal directions. Once the wavelet transform is found, the quadtree is computed by dividing the image into dyadic squares with variable sizes (refer to [3] for more information on computing the quadtree). For each square in the quadtree the optimal geometrical direction is computed by the minimization of a lagrangian (refer also to [3]). Then a projection of the wavelet coefficients along the optimal direction is performed [3]. Finally a 1D discrete wavelet transform is carried on the projected coefficients.
On figure 2 one can see, for the finest scale of the wavelet transform, the quadtree, and a zoom on the orientation of the linear flow on each dyadic square. Notice that the quadtree segmentation performs very

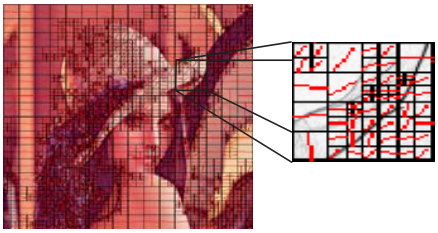

Fig. 2. Lenna image quadtree segmented

well in the area corresponding to edges.

3. ANISOTROPIC DIFFUSION: PERONA-MALIK FORMULATION

The aim of the diffusion algorithms is to filter the noise from an image by modifying the image via a PDE. Perona and Malik [1] replaced the classical isotropic diffusion equation with

$$\frac{\partial I(x,y,t)}{\partial t} = div\left[g\left(\|\nabla I\|\right)\nabla I\right] \tag{2}$$

Where $\|\nabla I\|$ is the gradient magnitude, and $g\left(\|\nabla I\|\right)$ is an edge stopping function satisfying $g(x) \to 0$ when $x \to \infty$ so that the diffusion is "stopped" across edges.
However, the Perona-Malik model meets several serious practical and theoretical difficulties. The first inconvenience is related to its sensitivity to noise. Assume an image carries strong noise. The Perona-Malik model will conserve the noise in the processing. Another difficulty arises from the existence of the local backward diffusion in the area where $\left(g\left(\|\nabla I\|\right)\nabla I\right) < 0$. There is no existent theory to support the uniqueness of the solutions of equation (2). Examples show that (2) is unstable in the sense that very close images could produce divergent solutions [5].
The multistructural tensor of Di Zenzo [6] allowed the extension of the Perona-Malik approach toward color or multispectral images. For a multichannel image $I = \left(I^1, I^2, ..., I^n\right)^T$ the structure tensor is given by

$$Q = \begin{pmatrix} I_x^T I_x & I_x^T I_y \\ I_y^T I_x & I_y^T I_y \end{pmatrix} \tag{3}$$

where superscript T indicates the transpose operation.
The extended Perona-Malik model for an m-valued image can be written as:

$$\begin{cases} \frac{\partial I_i}{\partial t} = div\left(g\left(\|Q\|\right)\nabla I_i\right) \\ I_i(x,y,0) = I_{i_0}(x,y) \qquad for \qquad i = 1,2.....,m \\ \left.\frac{\partial I_i}{\partial n}\right|_{\partial\Omega} = 0 \end{cases} \tag{4}$$

Where Ω is the image domain.

4. BANDELET-BASED ANISOTROPIC DIFFUSION

The Perona-Malik model regularizes the image gradient ∇I to reduce the influence of noise. The effectiveness of the regularization is therefore dependent on the type of noise. The motivation of this work is to make the anisotropic diffusion adjusted by the optimal geometrical direction in each square of the quadtree. For that purpose, a multiscale multistructural bandelet-based diffusion tensor for an m-valued image is defined by:

$$G_B^j = \left[\begin{array}{cc} \sum_{i=1}^{m}\left(\frac{\partial}{\partial x}B_{i,q}^j\cos\theta_i\right)^2 & \sum_{i=1}^{m}\frac{\partial}{\partial x}B_{i,q}^j\cos\theta_i\frac{\partial}{\partial y}B_{i,q}^j\sin\theta_i \\ \sum_{i=1}^{m}\frac{\partial}{\partial x}B_{i,q}^j\cos\theta_i\frac{\partial}{\partial y}B_{i,q}^j\sin\theta_i & \sum_{i=1}^{m}\left(\frac{\partial}{\partial y}B_{i,q}^j\sin\theta_i\right)^2 \end{array}\right]_{for \quad i=1,2,.....m} \tag{5}$$

The norm of G_B^j is defined in terms of its eigenvalues λ_+ and λ_-, $||G_B|| = \sqrt{\lambda_+ + \lambda_-}$. The angle θ_i represents the angle of the optimal direction of the geometrical flow. j is the scale of the 2D wavelet transform. $B_{i,q}^j$ is the corresponding bandelet coefficient at the square number q. The squares in the quadtree are numbered from top to bottom and from left to right. Figure 3 shows the norms of the multiresolution tensor of Di Zenzo (Fig. 3(b)) and the norm of the multiscale multistructure tensor defined in (5) (Fig. 3(c)) of the noisy 'Lenna' image.
It is clear that the norm of the structure tensor defined in (5) provided a better edge characterization. We should notice here that the singularities of the image edges are well characterized with small fitted squares (Fig. 2). Furthermore, noise pixels will be represented by the maximal geometrical flow driven by the non-noisy pixels in the corresponding dyadic square. Thus, the noisy pixels have no influence on the geometrical flow representation. As a result, the norm of the structural tensor proposed in (5) represents only the pixels with a maximal intensity change, i.e., the edges. Another interesting advantage is that the geometry of the image is summarized with local clustering of similar geometric vectors. Therefore, the homogeneous areas are taken from a quadtree structure. As a result, the blurring is reduced since the boundaries between the different homogeneous image areas are conserved.
It is to be noted that for a each dyadic square in the quadtree we have a different structure tensor according to the direction of the geometrical flow.
The bandelet-based anisotropic diffusion is therefore defined by:

$$\begin{cases} \frac{\partial I_i}{\partial t} = div\left(g\left\|G_B^j\right\|\right)\tilde{\nabla} I_i \\ I_i(x,y,0) = I_{i_0}(x,y) \\ \left.\frac{\partial I_i}{\partial n}\right|_{\partial\Omega} = 0 \end{cases} \tag{6}$$

Where g is the edge stopping function and $\tilde{\nabla} I_i$ is the directional gradient with respect to the direction of the flow. Common diffusiv-

(a) Noisy Lenna Image

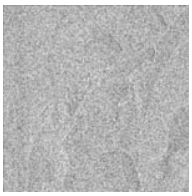

(b) Norm of the Di Zenzo tensor

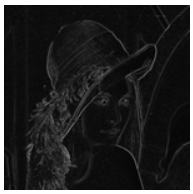

(c) Norm of the structure tensor defined in (5)

Fig. 3. Norm of different multistructural tensor

ity functions or edge stopping functions are proposed by Perona [1], German and Reynolds [7], Aubert et al. [8] and Saint-Marc et al [9]. For example, the one proposed by Perona et Malik is defined by:

$$\exp\left(-\left(\frac{\nabla I}{k}\right)^2\right)$$

The k parameters in these functions, also called edge threshold parameter, controls the shape of the diffusivity function, balancing the degrees of inter-region smoothing and edge enhancement in the diffusion process. Perona and Malik proposed to compute the histogram and then let k equals to 90% of the integral of the histogram. Since the obtained representation by using (5) is an accumulation of gradients, this results in an enlarged edge stopping value that improves noise reduction while preserving edge structures. Actually, the k parameter is computed as follows.
It can be shown that:

$$\sigma^2 \sqrt{\lambda_v^+ + \lambda_v^-} \approx N\sigma_v^2 \tag{7}$$

with N the number of pixels in the image and σ_v^2 the noise variance at scale v of the 1D wavelet transform used in the computation of the bandelet coefficients. σ_v^2 is given by:

$$\sigma_v^2 = \|\psi_v\|^2 \sigma^2 \tag{8}$$

where σ^2 is the noise variance of the image, ψ is the mother wavelet used to compute the wavelet transform of the image, and $\|\psi_v\|^2$ designates its norm . The k parameter is made proportional to σ_v:

$$k = c\sqrt{N}\sigma_v \tag{9}$$

Where c is a constant.

5. EXPERIMENTAL RESULTS

This section is devoted to comparing the Bandelet-based anisotropic diffusion scheme that is presented in this paper with previous work on image restoration.
For that purpose, the noisy image shown in figure 4(b) is processed by equation (6) as well as by the Perona-Malik scheme. The noisy image is obtained by adding a white gaussian noise to the image of figure 4(a).

(a)

(b)

Fig. 4. Original image and the noisy image (SNR=27.21dB) obtained by adding a white gaussian noise

In figures 5(a) and 5(b), the results obtained by filtering the noisy images (fig. 4(b)) by the Perona-Malik approach (equation 4) and the Bandelet-based regularization (equation 6) are shown respectively.
The noisy image of figure 4(b) is also processed with the edge enhancement diffusion (EED) [10], the coherence enhancement diffusion (CED) [11], the Tikhonov diffusion (TD), the color total variation schemes (CTV) and the undecimated wavelet coefficients hard thresholding and soft thresholding. The results are shown in figures 6. The problem with wavelet coefficient thresholding is that setting coefficients to zero leads to smooth image (Fig. 6(f)) and destroy details which cause blur and artifacts (Fig. 6(e)).

(a)

(b)

Fig. 5. Filtered image obtained by: (a) The Perona-Malik approach (SNR=31.59dB), (b) the Bandelet-based approach (SNR=32.9dB)

Compared to the other schemes, the Bandelet-based anisotropic diffusion showed better details preserving, less blurring and better image restoration.
The quality of the filtered images is also evaluated using $CIEDE2000$ color difference equations [12]. The $CIEDE2000$ evolved from traditional colorimetry and color difference calculations is tested using several psychophysical datasets. The color differences between the original image (Fig. 4(a)) and each of the filtered images obtained using different denoising schemes are shown in figure 7. The PDE bandelet-based approach showed the lowest color difference and therefore it approaches the original image more than the other denoising techniques. Therefore, it respects the colorimetric characteristics of the original image. We have also processed the noisy image (Fig. 4(b)) with the wavelet-based methods proposed by Scheunders in [13] and Pižurica et al. in [14]. However, the proposed Bandelet-based diffusion achieved better SNR (the SNR of the former is 31.97 dB while that of the latter is 32.04 dB) as well as lowest $CIEDE2000$ color differences.

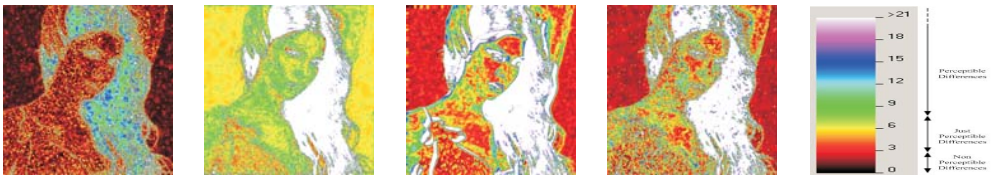

(a) (b) (c) (d) (e)

Fig. 7. $CIEDE2000$ color difference between the original image and the filtered image obtained by: (a) bandelet based approach, (b) Wavelet hard thresholding, (c) Perona and Malik approach (d)Color Total Variation

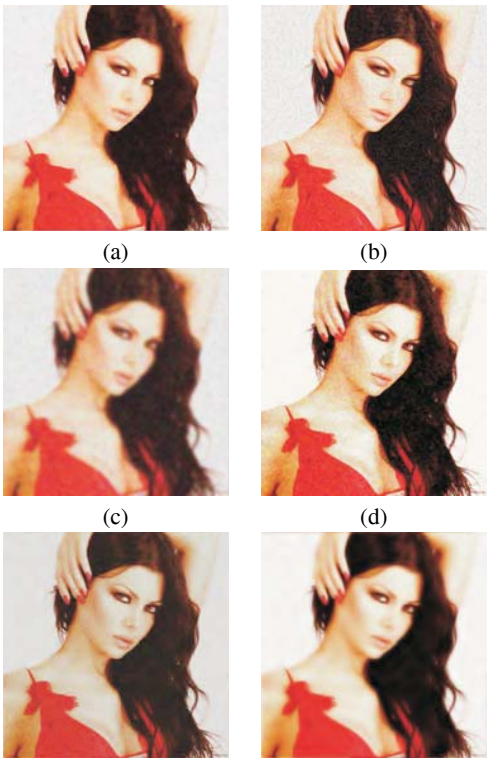

(a) (b) (c) (d) (e) (f)

Fig. 6. Filtered image obtained by: (a) EED (SNR=29.058dB), (b) CED (SNR=29.11dB), (c) (TD) (SNR=32.11dB), (d) (CTV) (SNR=28.76dB), (e) Wavelet hard thresholding(SNR=38.95dB) and (f) wavelet soft thresholding(SNR=31.28dB)

6. CONCLUSION

In this paper, a bandelet-based anisotropic diffusion is described. It uses a multiscale structure tensor that is computed from the bandelet coefficients and the direction of the geometrical flow of the image being processed. The introduced structure tensor provides a better edge characterization than the structure tensor of Di Zenzo. The bandelet-based diffusion provides a better edge preserving and less blurring in the processed image. The proposed scheme is compared with earlier anisotropic diffusion schemes and with wavelet thresholding techniques. A future perspective could be to extend the proposed scheme to the regularization of surfaces of higher dimensional images.

7. REFERENCES

[1] Perona P. and Malik J., "Scale-space and edge detection using anisotropic diffusion," *IEEE Trans. Pattern Anal. Machine Intell.*, vol. 12, no. 7, pp. 629–639, 1990.

[2] E. Le Pennec and S. Mallat, "Sparse geometric image representation with bandelets," *IEEE Trans. Image Processing*, vol. 14, no. 4, pp. 423–438, 2005.

[3] G. Peyre and S. Mallat, "Surfave compression with geometrical bandelets," *ACM Transactions on Graphics*, vol. 14, no. 3, 2005.

[4] Peyre G., *Geometrie multi-chelles pour les images et les textures*, Phd thesis, Ecole Polytechnique, December 2005.

[5] Tannenbaum A. Yu-Li You and Kaveh M., "Behavioral analysis of anisotropic diffusion in image processing," *IEEE Trans. Med. Imaging*, vol. 5, pp. 1539–1553, 1996.

[6] DiZenzo S., "A note on the gradient of multi images," *Computer Vision Graphics and Image processing*, vol. 33, no. 1, pp. 116–125, 1986.

[7] S. German and G. Reynolds, "Contrained restoration and the recovery of discontinuities," *IEEE transactions on pattern analysis machine intelligence*, vol. 14, 1992.

[8] Gilles Aubert and Luminita Vese, "A variational approach in image recovery," *SIAM journal of numerical analysis*, vol. 34, no. 5, pp. 1948–1979, 1997.

[9] J. Chen P. Saint-Marc and G. Medioni, "Adaptive smoothing: A general toll for early vision," *IEEE transactions on pattern analysis machine intelligence*, vol. 13, no. 6, pp. 514–529, 1991.

[10] Weickert J., "Scale space properties of nonlinear diffusion filtering with a diffusion tensor," Technical report, University of Kaiserslautern, October 1994.

[11] Lopez A. Weickert J., Haar Romeny B. M. and Van Enk W. J., "Orientation analysis by coherence-enhancing diffusion," in *Proc. Symp. Real World Computing*, 1997, pp. 96–103.

[12] G. M. Johnson and M. D. Fairchild, "A top down description of s-cielab and ciede2000," *Color Res. Appl.*, vol. 27, 2002.

[13] P. Scheunders, "Wavelet thresholding of multivalued images," *IEEE Trans. Image Processing*, vol. 13, no. 4, pp. 475–483, 2004.

[14] A. Pisurica and W. Philips, "Estimating probability of presence of a signal of interest in multiresolution single and multiband image denoising," *IEEE Trans. Image Processing*, vol. 15, no. 3, pp. 654–656, 2006.